

PACS numbers: 42.79.Jq
DOI: 10.1070/QE2004v034n03ABEH002627

Competition of modes in an optically heterodyned acoustooptic generator

V.I. Balakshy, I.M. Sinev

***Abstract*. An acoustooptic generator in which the feedback signal is produced using optical heterodyning is studied theoretically and experimentally. The development of oscillations in this system is analysed by computer simulations. It is shown that the competition of modes caused by nonlinearity of the acoustooptic interaction can result in the degeneration of the generation spectrum and the establishment of a single-mode regime. The dependence of the generator linewidth on the parameters of the system is studied.**

Keywords: *acoustooptic interaction, optoelectronic generator, optical heterodyning, mode competition.*

1. Introduction

Acoustooptic (AO) systems with a feedback is a new class of devices which expand substantially the scope of problems of optical data processing that can be solved by AO methods [1, 2]. The feedback in these systems is hybrid: the output signal of an AO cell is transformed to the electric signal, which in turn controls the amplitude [3 – 6] or frequency [7 – 9] of an acoustic wave propagating in the cell. The AO systems with the feedback are essentially nonlinear. The feedback can be effected via diffraction maxima of different orders, resulting in different types of nonlinearity. It is also necessary to take into account a finite transit time of the acoustooptic signal in the AO cell, which is, as a rule, much longer than the time of signal propagation in the electric circuit of the system. The behaviour of the feedback AO systems is extremely varied. Oscillations of different types (including chaotic) can be excited in them, and bistable and multistable regimes with the optical or electric switching of states can appear [6, 8].

An AO generator in which a feedback signal is produced by the method of optical heterodyning has especially interesting properties [10 – 12]. This system does not contain a separate electric oscillator, as in other devices of a similar type. Acoustic oscillations are excited by supplying the optical heterodyning signal to the piezoelectric transducer of the AO cell. The AO generator has a number of unique properties. Oscillations of different physical nature (electric, acoustic, and optical) can be excited in it, which are interrelated and can transform to each other. Many parameters of the AO generator are similar to those of a laser. As in a laser, single-mode and multimode regimes are possible in the AO generator, as well as typical laser effects such as mode competition and mode locking.

In this paper, we focus our attention on the process of establishment of oscillations in the AO generator, the mode competition effect, and the influence of variations in the system parameters on the characteristics of the generation spectrum.

V.I. Balakshy, I.M. Sinev Department of Physics, M.V. Lomonosov Moscow State University, Vorob'evy gory, 119992 Moscow, Russia

Received 29 July 2003
Kvantovaya Elektronika **34** (3) 277 – 282 (2004)
Translated by M.N. Sapozhnikov

2. Experimental results

The scheme of the AO generator is shown in Fig. 1. Radiation of laser (*1*) is split in beamsplitter cube (*2*) into two beams, one of which is used as a signal beam and another as a reference beam. The signal beam propagating through AO cell (*3*) diffracts by ultrasound. Due to the Doppler effect, the light frequency ν shifts by the ultrasonic frequency f. The reference beam is made coincident with the first diffraction order of the signal beam. The interference of these beams produces beats at the ultrasonic frequency f, which are detected with photodetector (*4*). The output electric signal of the photodetector is amplified in amplifier (*5*) and is fed to piezoelectric transducer (*6*) of the AO cell, which excites an acoustic wave. If the feedback is sufficiently strong, harmonic oscillations can appear in the system.

The system shown in Fig. 1 was realised experimentally [12]. A 0.63-μm helium – neon laser was used in the setup.

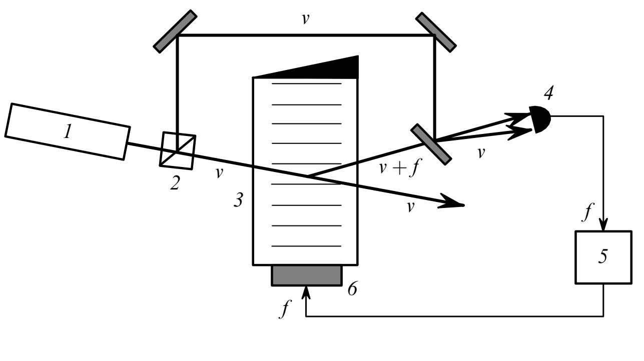

Figure 1. Principal scheme of the AO generator: (*1*) laser; (*2*) beamsplitter; (*3*) AO cell; (*4*) photodetector; (*5*) amplifier; (*6*) piezoelectric transducer.

The laser beam was split in a polarisation cube into the reference and signal beams with mutually orthogonal polarisations. Light was detected with an avalanche photodiode. The signal passed in the feedback circuit through a cascade of amplifiers with the total gain $\varkappa = 3 \times 10^4$. The maximum amplitude of the output signal of the amplifier cascade was approximately 22 V.

We used in the system the AO cell cut from a paratellurite crystal (TeO_2). This crystal has a strong optical and acoustic anisotropy and an extremely high AO figure of merit, which provides the efficient diffraction [1]. A shear slow acoustic wave was excited in the cell at an angle of 4° to the [110] axis in the $(1\bar{1}0)$ plane. The AO interaction in the cell represented anisotropic diffraction accompanied by a change in the polarisation of light. For interference to occur, radiation of the same polarisation is required. This explains the use of the polarisation beamsplitter cube at the system entrance.

As was shown in Ref. [11], the behaviour and parameters of the AO generator are similar to those of a laser. The distance z_0 from the piezoelectric transducer to the region of the AO interaction plays the role of the laser resonator. This distance specifies the frequency interval between modes

$$\Delta f = \frac{V}{z_0}, \qquad (1)$$

where V is the sound speed in the cell. The number of generated modes is determined by the angular range of optical heterodyning, which plays the same role as the gain line profile of the laser. When the light beam propagates near the transducer, only one mode falls within the gain line profile, and only single-mode generation is possible. As z_0 increases, the number of modes within the gain profile increases proportionally.

We observed in our experiments both single-mode and multimode generation at frequencies near 30 MHz. Figure 2 shows oscillograms obtained with the help of a spectrum analyser connected to the amplifier output. The oscillograms were obtained for the same adjustment of the system, when 17 modes fell within the gain profile. The single-mode regime was more stable, which indicates that the competition of modes takes place in the AO generator. One of the possible mechanisms of such a competition is the multifrequency AO interaction appearing in the case of efficient diffraction [13]. Below, we consider this effect theoretically.

Similarly to a laser, we can expect that mode locking also exists in the AO generator. To observe this effect, we placed an electrooptical modulator in the reference beam. For an arbitrary frequency of the external perturbation, we observed modulated harmonic oscillations with the depth of modulation not exceeding 10 % (Fig. 3a). However, when the external-perturbation frequency was equal to the intermode beat frequency Δf, the picture changed substantially. The AO generator began to work in the pulse regime (Fig. 3b). Mode locking also occurred at frequencies $2\Delta f$ and $3\Delta f$.

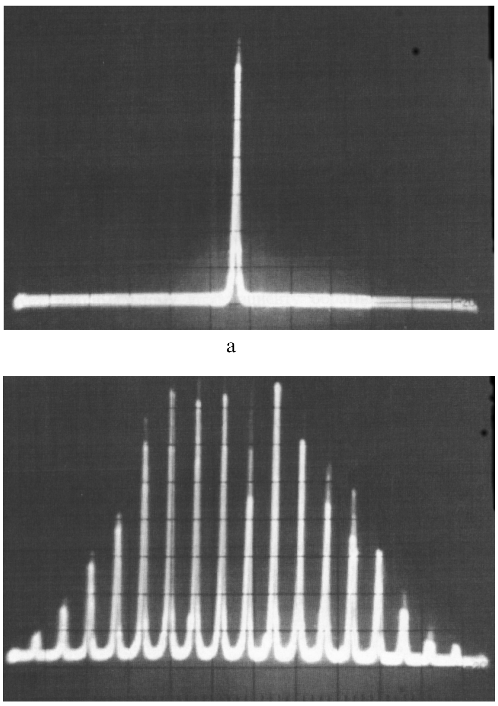

a

b

Figure 2. Single-mode (a) and multimode (b) generation spectra.

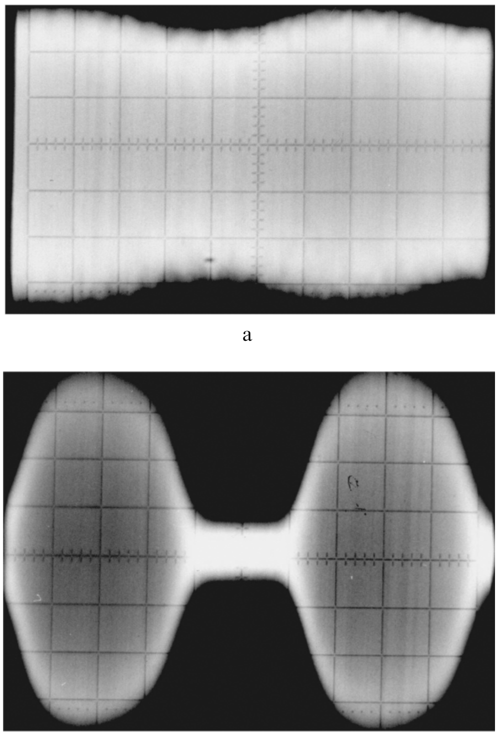

a

b

Figure 3. Oscillograms of the output signal of the generator in the case when the modulation frequency is outside the mode-locking band (a) and in the mode-locking regime (b).

3. Basic relations

We will analyse the operation of the system under study by the spectral method [1, 2]. Let us assume for simplicity that the signal and reference beams are Gaussian beams with the width d in the AO interaction plane xz and the width b in the orthogonal direction. The signal beam passes through the AO cell at the angle ϑ_0 at the distance z_0 from a piezoelectric transducer. By expanding the incident signal beam in the spectrum in plane waves, we obtain the expression

$$U_{\rm i}(\vartheta_{\rm i},\psi)=\frac{\pi}{4}u_0 db\exp\left[-\frac{\pi^2 n^2 d^2}{4\lambda^2}(\vartheta_{\rm i}-\vartheta_0)^2\right]$$

$$\times\exp\left(-\frac{\pi^2 n^2 b^2}{4\lambda^2}\psi^2\right)\exp\left[-{\rm i}\frac{2\pi n}{\lambda}z_0(\vartheta_{\rm i}-\vartheta_0)\right], \quad (2)$$

where u_0 is the incident radiation amplitude; $\vartheta_{\rm i}$ and ψ are angles in the planes xz and xy, respectively; and n is the refractive index of the cell material. Because the principle of superposition of light fields is valid for the AO interaction, each of the components of spectrum (2) diffracts in the acoustic field independently of the other components. Let us assume that the adjustment of the system is optimal, i.e., the angles of incidence of the signal (ϑ_0) and reference ($\vartheta_{\rm r}$) beams satisfy the Bragg condition for some ultrasonic frequency

$$f_{\rm r}=\frac{nV}{\lambda}(\vartheta_{\rm r}-\vartheta_0). \quad (3)$$

Because a great number of modes can be excited in the generator, we consider the AO interaction for the equidistant frequency set f_0, $f_0\pm\Delta f$, $f_0\pm 2\Delta f$, ...

In the usual Bragg regime of diffraction from monochromatic sound with the frequency f_0, light diffracts from the zero order with the frequency ν to the first order, where the frequency is $\nu+f_0$, and back. When the sound field contains two frequencies (f_0 and $f_0+\Delta f$), light first diffracts from the zero order to two first orders with frequencies $\nu+f_0$ and $\nu+f_0+\Delta f$. Upon back diffraction, three zero orders with frequencies ν, $\nu+\Delta f$, and $\nu-\Delta f$ appear. Then, light diffracts to the four first orders with frequencies $\nu+f_0$, $\nu+f_0+\Delta f$, $\nu+f_0-\Delta f$, and $\nu+f_0+2\Delta f$, etc. Thus, due to multiple diffraction in a strong acoustic field, not two light beams appear, as in the usual Bragg regime, but a theoretically infinite number of beams in the zero and first diffraction orders [13]. Taking into account this peculiarity, we will assume that an electric signal with the equidistant spectrum of the type

$$u(t)=\sum_{i=0,\pm1,\pm2,...}u_{0i}\sin(2\pi f_i t+\Phi_i) \quad (4)$$

is fed to the piezoelectric transducer, where u_{0i} and Φ_i are the amplitudes and phases of harmonic components, respectively, and $f_i=f_0+i\Delta f$.

By generalising the equations of coupled modes to the case of a multifrequency acoustic field, we obtain the system of equations for the complex amplitudes of diffracted waves

$$2\frac{{\rm d}C_{1i}}{{\rm d}x}=-\sum_k q_k C_{0\,i-k}\exp\left[-{\rm i}(\eta_{i-k\,i}x-\Phi_k)\right],$$
$$2\frac{{\rm d}C_{0m}}{{\rm d}x}=\sum_k q_k C_{1\,m+k}\exp\left[{\rm i}(\eta_{m\,m+k}x-\Phi_k)\right], \quad (5)$$

where C_{jm} is the relative amplitude of light in the mth maximum of the jth diffraction order ($j=0$, 1) and q_k are the coefficients of the AO coupling, which are proportional to the corresponding amplitudes u_{0k} ($k=0,\pm1,\pm2,...$). The coefficients η_{im} of the phase mismatch in an anisotropic medium are described by the expression

$$\eta_{im}=\frac{2\pi}{\lambda}(n_0-n_1)+\frac{\pi}{\lambda}(f_0+m\Delta f-i\Delta f)$$
$$\times\left[2\vartheta_0+\frac{\lambda}{Vn}(f_0+m\Delta f+i\Delta f)\right], \quad (6)$$

where n_0 and n_1 are the refractive indices for the waves of the zero and first diffraction orders, respectively. The solution of system (5) for the AO interaction region $0\leqslant x\leqslant l$ with the natural boundary conditions $C_{1i}(0)=0$ and $C_{0m}(0)=\delta_{0m}$ gives a set of complex quantities $C_{1i}(l)$ and $C_{0m}(l)$. Their moduli determine the amplitudes of diffracted waves, while the arguments determine the additional phase shifts produced during the AO interaction.

The spectrum of diffracted light has the form

$$U_{\rm d}(\vartheta_{\rm d},\psi)=\frac{\pi}{4}u_0 db\exp\left(-\frac{\pi^2 n^2 b^2}{4\lambda^2}\psi^2\right)$$
$$\times\sum_i\left\{\exp({\rm i}2\pi f_i t)\exp\left[-\frac{\pi^2 n^2 d^2}{4\lambda^2}\left(\vartheta_{\rm d}-\frac{K_i}{k}-\vartheta_0\right)^2\right]\right.$$
$$\left.\times\exp\left[-{\rm i}\frac{2\pi n}{\lambda}z_0\left(\vartheta_{\rm d}-\frac{K_i}{k}-\vartheta_0\right)\right]C_{1i}\right\}, \quad (7)$$

where $k=2\pi n/\lambda$ and $K_i=2\pi f_i/V$ are the wave numbers of light and sound. The signal beam diffracted to the first order interferes on the photodetector surface with the reference beam, whose spectrum can be written in the form

$$U_{\rm r}(\vartheta_{\rm d},\psi)=\frac{\pi}{4}u_{\rm r} db\exp\left[-\frac{\pi^2 n^2 d^2}{4\lambda^2}(\vartheta_{\rm d}-\vartheta_{\rm r})^2\right]$$
$$\times\exp\left(-\frac{\pi^2 n^2 b^2}{4\lambda^2}\psi^2\right)\exp\left[-{\rm i}\frac{2\pi n}{\lambda}z_0(\vartheta_{\rm d}-\vartheta_{\rm r})\right]. \quad (8)$$

The angular distribution of the light intensity on the photodetector is described by the expression

$$|U_{\rm d}(\vartheta_{\rm d},\psi)+U_{\rm r}(\vartheta_{\rm d},\psi)|^2=|U_{\rm d}|^2+|U_{\rm r}|^2+2{\rm Re}(U_{\rm d}U_{\rm r}^*). \quad (9)$$

The last (interference) term in the right-hand side of this expression describes the change in the intensity at the ultrasonic frequency f_i. It is clear from this that the output ac electric signal from the amplifier fed to the piezoelectric transducer is proportional to the integral from this term over the entire surface of the photodetector. Finally, by introducing the powers P_0 and $P_{\rm r}$ of the incident beams, we obtain the signal on the transducer

$$u_{\rm fb}(t)=2(P_0P_{\rm r})^{1/2}\mu\varkappa\sum_i\left\{\exp\left[-\frac{\pi^2 n^2 d^2}{8\lambda^2}\left(\vartheta_0-\vartheta_{\rm r}+\frac{K_i}{k}\right)^2\right]\right.$$
$$\left.\times|C_{1i}|\cos\left[2\pi f_i t+\frac{2\pi n}{\lambda}z_0\left(\vartheta_0-\vartheta_{\rm r}+\frac{K_i}{k}\right)+\arg C_{1i}+\varphi\right]\right\}, \quad (10)$$

where μ is the sensitivity of the photodetector, and the parameter φ takes into account the possible phase shift between the reference and signal waves.

Excitation of oscillations in the AO generator corresponds to the regime of a low diffraction efficiency. In this case, the AO interaction between modes is absent and the solution of system (5) has a simple form

$$C_{1i} = -\frac{q_i l}{2}\operatorname{sinc}\frac{\eta_{0i} l}{2\pi}\exp\left[-\mathrm{i}\left(\frac{\eta_{0i} l}{2} - \Phi_i\right)\right]. \quad (11)$$

By substituting (11) into (10) and comparing the obtained expression with (4), we find the condition for self-excitation of oscillations for each frequency f_i. It is necessary to take into account that $q_i l = \alpha u_{0i}$, where α is the proportionality coefficient determined by the parameters of the transducer and the properties of the AO medium. As a result, we have

$$B(P_0 P_\mathrm{r})^{1/2} G(f_i) > 1, \quad (12)$$

where $B = \mu\varkappa\alpha$ is the feedback coefficient. The condition of self-excitation in form (12) was earlier obtained in Ref. [11]. The function $G(f_i)$ is determined by the expression

$$G = \exp\left[-\frac{\pi^2 d^2}{8V^2}(f_i - f_\mathrm{r})^2\right] \times \operatorname{sinc}\left\{\frac{l}{V}(f_i - f_\mathrm{r})\left[\vartheta_0 + \frac{\lambda}{2nV}(f_i + f_\mathrm{r})\right]\right\}. \quad (13)$$

This function describes the angular selectivity of the AO interaction [factor sinc (...)] and of the optical heterodyning [factor exp (...)]. This function, which can be treated as the gain line of the AO generator, determines first of all the frequencies f_i that will be excited in the system. In the Raman–Nath regime, when the selectivity of the AO interaction disappears, the gain profile is described by the expression

$$G = \exp\left[-\frac{\pi^2 d^2}{8V^2}(f_i - f_\mathrm{r})^2\right], \quad (14)$$

which shows that the lowest self-excitation threshold is obtained for the spectral component of the acoustic field that gives the diffracted beam coaxial with the reference beam.

As in a laser, another factor determining the spectrum of the generated signal is the self-consistence of the signal, which is characterised by the condition of the phase balance. This condition is obtained from expressions (10) and (4):

$$f_i = f_\mathrm{r} + \frac{V}{z_0}\left(i + \frac{\varphi}{2\pi}\right). \quad (15)$$

The number of generated modes can be controlled by changing either the gain $\varkappa$ or distance z_0. This number is minimal when the light beam propagates near the transducer. When the phase shift φ changes, the intermode interval Δf does not change, while the mode 'comb' shifts with respect to the gain profile.

The AO generator has a high sensitivity to the angular and linear displacements of the incident or reference beam, as well as to variations in the phase shift φ. It is important that the angular and linear coordinates are transformed here to the frequency, i.e., to the physical quantity measured at present with the highest accuracy. Relation (15) gives the following expressions for the transformation coefficients in angle (χ_ϑ), coordinate (χ_z), and phase (χ_φ):

$$\chi_\vartheta = \frac{\partial f}{\partial \vartheta} = \frac{nV}{\lambda}, \quad \chi_z = \frac{\partial f}{\partial z} = \frac{V}{z_0^2}, \quad \chi_\varphi = \frac{\partial f}{\partial \varphi} = \frac{V}{2\pi z_0}. \quad (16)$$

These coefficients for the paratellurite cell used in our experiments are $\chi_\vartheta = 0.67$ MHz angl. min^{-1}, $\chi_z = 0.64$ MHz mm^{-1}, and $\chi_\varphi = 0.1$ MHz rad^{-1}.

4. Computer simulation

We studied processes proceeding in the AO generator during the development of oscillations by the method of computer simulation. For this purpose, we wrote a software simulating the development of oscillations in the stroboscopic approximation, i.e., the states of the system were calculated at intervals τ equal to the transit time of the acoustic signal from the piezoelectric transducer to the region of AO interaction: $\tau = z_0/V = 1/\Delta f$.

It is convenient to perform numerical calculations using dimensionless quantities. Then, system (5) takes the form

$$2\frac{\mathrm{d}C_{1i}}{\mathrm{d}X} = -\sum_k A_k C_{0\,i-k}\exp\left[-\mathrm{i}(R_{i-k\,i}X - \Phi_k)\right],$$
$$2\frac{\mathrm{d}C_{0m}}{\mathrm{d}X} = \sum_k A_k C_{1\,m+k}\exp\left[\mathrm{i}(R_{m\,m+k}X - \Phi_k)\right], \quad (17)$$

where $X = x/l$; $A_k = q_k l$ are the Raman–Nath parameters ($k = 0, \pm 1, \pm 2, \ldots$). The dimensionless mismatches $R_{im} = \eta_{im} l$ are described by the expression

$$R_{im} = \frac{Q}{2}\left\{\pm F^{*2} + [F_0 + (m-i)\Delta F] \times\left[F_0 + (m+i)\Delta F - 1 \mp F^{*2}\right]\right\}, \quad (18)$$

where $Q = 2\pi\lambda l f_\mathrm{r}^2/(nV^2)$ is the Klein–Cook parameter; $F_0 = f_0/f_\mathrm{r}$; $\Delta F = \Delta f/f_\mathrm{r}$; and $F^* = f^*/f_\mathrm{r}$ is the characteristic frequency of anisotropic AO scattering [1]. The plus and minus signs correspond to the different branches of anisotropic diffraction. In the case of isotropic diffraction, we should set $F^* = 0$. Similarly, expression (10) can be reduced to the form

$$u_\mathrm{fb}(t) = 2(P_0 P_\mathrm{r})^{1/2}\mu\varkappa\sum_i\left\{\exp\left[-\frac{\pi^2 D^2}{8}(F_0 + i\Delta F - 1)^2\right] \times |C_{1i}|\cos\left[2\pi f_i t + 2\pi Z_0(F_0 + i\Delta F - 1) + \arg C_{1i} + \varphi\right]\right\}, \quad (19)$$

where $D = d f_\mathrm{r}/V$; $Z_0 = z_0 f_\mathrm{r}/V$.

The algorithm of calculations consists in the following. We assume that at the initial instant $t = 0$ the system contains noise oscillations with the same amplitude in the entire frequency range of interest. By specifying the feedback coefficient B, we could determine the frequencies f_i of modes for which the self-excitation condition (12) is fulfilled. For these modes, system of equations (17) was solved and the amplitudes $u_{0i}^{(1)}$ and phases $\Phi_i^{(1)}$ of the harmonic components of signal (4) were calculated from (19) at the first step of the iteration process. The calculation of system (17) for new values of A_k and Φ_k gave the amplitudes $C_{1i}^{(1)}$, characterising the state of the system for $t = \tau$. Then, the iteration process was repeated and the states of the system at instants $t = 2\tau$, $3\tau, \ldots$ were calculated in this way.

5. Results of calculations

Figure 4 illustrates formation of the mode structure in the AO generator. Here, the oscillation spectra are presented for different instants of time. Straight line (*1*) corresponds to the initial state with the uniform spectrum. The mode structure appears after the first passage of a signal in the feedback circuit [curve (*2*)]: the signal increases at frequencies f_i satisfying relation (15). The phase shift φ was chosen in the calculation so that the mode with frequency f_0 was located at the centre of the gain profile; in this case, $f_0 = f_r$. This mode experiences the highest amplification and, therefore, increases faster than other modes.

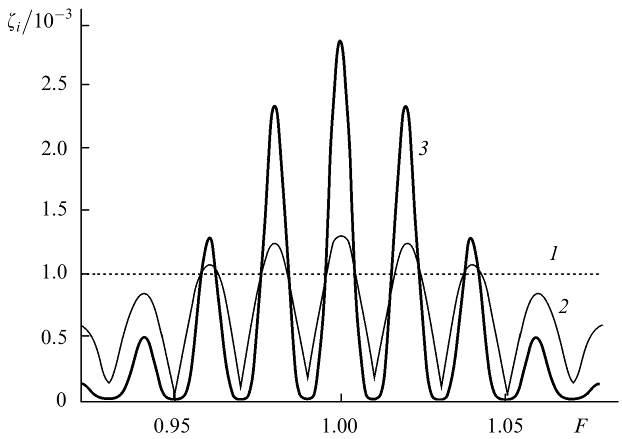

Figure 4. Formation of the mode structure in the generator: oscillation spectra at instants $t = 0$ (*1*), $t = \tau$ (*2*), $t = 5\tau$ (*3*) (ζ is the diffraction efficiency, $F = f/f_r$).

The oscillation process is developed in such a way until the total efficiency of diffraction of light from all acoustic modes achieves 5 % – 10 %. The situation changes in the regime of high diffraction efficiency. The central mode, which is in the most favourable conditions, 'captures' a greater part of the incident light. As a result, the amplitudes of other modes pass through the maximum and decrease to zero. Therefore, the mode competition in the system leads to the establishment of single-mode generation. This is illustrated in Fig. 5 where the time dependences of the diffraction efficiency ζ_i for each mode are shown. Curve (*1*) demonstrates the development of the stationary regime for the central mode. Curves (*2*) and (*3*) correspond to the nearest symmetrically spaced modes with indices $i = \pm 1$ and ± 2, respectively. The calculation was performed for real values of the parameters: $Q = 10$, $D = 10$, $Z_0 = 100$. The value $\alpha = 1.3$ B^{-1} was taken from the experiment.

Curve (*1*) in Fig. 6 shows the dependence of the diffraction efficiency ζ_0 in the stationary regime on the integrated feedback coefficient $\eta = B(P_0 P_r)^{1/2}$. As η increases, oscillations are excited above the threshold value $\eta_{th} = 1$. Because the theory was developed for the Bragg regime, the diffraction efficiency can achieve 100 %. The corresponding feedback coefficient is equal to 1.6. As η further increases, the diffraction efficiency decreases and the system passes to the regime of stochastic oscillations.

To estimate the outlook for practical applications of the AO generator, it is important to know the generation linewidth δf. It can be found from the setting time δt of oscillations because $\delta f \delta t \approx 1$. Curve (*2*) in Fig. 6 shows the dependence of the line Q factor $1/\delta F = f_r/\delta f$ on the coefficient η. The narrowest lasing line is obtained near the threshold, where its relative width can be $10^{-2} - 10^{-3}$ at the relative width of the gain profile equal to $1 - 0.1$. The line Q factor increases with the distance z_0.

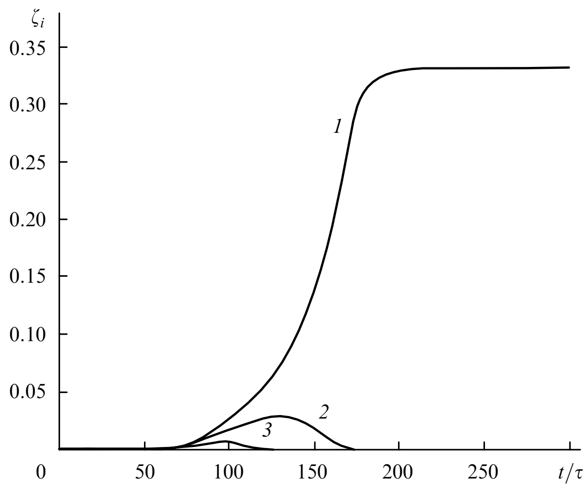

Figure 5. Transient process in the development of oscillations in the generator for the central mode (*1*) and side modes with indices $i = \pm 1$ (*2*) and ± 2 (*3*).

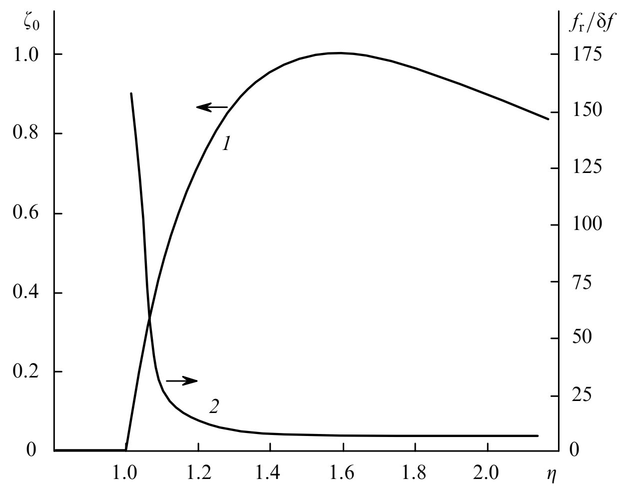

Figure 6. Dependences of the diffraction efficiency in the stationary regime (*1*) and of the generation line Q factor (*2*) on the integrated feedback coefficient.

6. Conclusions

We have studied theoretically and experimentally the AO generator in which the feedback signal is produced by the method of optical heterodyning. We have found that both single-mode and multimode lasing can occur in this system. The development of oscillations in the AO generator has been studied by the method of computer simulation. It is shown that, when the diffraction efficiency achieved 5 % – 10 %, the mode competition appeared due to the nonlinear AO interaction, resulting in single-mode generation. The diffraction efficiency in the stationary state depends on the feedback coefficient and can achieve 100 % in the Bragg regime. The dependence of the spectral width of the generated mode on the system parameters has been analysed.

The AO generator has a high sensitivity to the variation in its parameters. In fact, this generator is the Mach–Zehnder interferometer with the positive feedback. The width of the generator line is two–three orders of magnitude narrower than the pass band of a usual interferometer. Therefore, we can expect that the sensitivity of measurements performed with the help of the Mach–Zehnder interferometer will increase correspondingly.

Acknowledgements. This work was supported by the Russian Foundation for Basic Research (Grant No. 02-07-90448). The authors thank V.Ya. Molchanov for placing the AO cell at their disposal.

References

1. Balakshy V.I., Parygin V.N., Chirkov L.E. *Fizicheskie osnovy akustooptiki* (Physical Foundations of Acoustooptics) (Moscow: Radio i Svyaz', 1985).
2. Parygin V.N., Balakshy V.I. *Opticheskaya obrabotka informatsii* (Optical Data Processing) (Moscow: Izd. Moscow State University, 1987).
3. Jerominek H., Delisle C., Pomerleau J.Y.D., Tremblay R. *Can. J. Phys.*, **63**, 227 (1985).
4. Poon T.-C., Cheung S.K. *Appl. Opt.*, **28**, 4787 (1989).
5. Balakshy V.I., Kazaryan A.V., Molchanov V.Ya., Ming Hai. *Proc. SPIE Int. Soc. Opt. Eng.*, **1731**, 303 (1992).
6. Balakshy V.I., Kazaryan A.V., Molchanov V.Ya. *Radiotekhn. Elektron.*, **37**, 1140 (1992).
7. Balakshy V.I., Kazaryan A.V. *Proc. SPIE Int. Soc. Opt. Eng.*, **2430**, 292 (1994).
8. Balakshy V.I., Kazaryan A.V., Li A.A. *Kvantovaya Elektron.*, **22**, 975 (1995) [*Quantum. Electron.*, **25**, 940 (1995)].
9. Balakshy V.I., Kazaryan A.V. *Opt. Eng.*, **38**, 1154 (1999).
10. Babkina T.V., Grigor'yants V.V., Ili'in Yu.B., Prokof'ev V.A. *Kvantovaya Elektron.*, **18**, 259 (1991) [*Sov. J. Quantum. Electron.*, **21**, 230 (1991)].
11. Balakshy V.I., Nagaeva I.A. *Kvantovaya Elektron.*, **23**, 261 (1996) [*Quantum. Electron.*, **26**, 254 (1996)].
12. Balakshy V.I., Emelianov S.V. *Proc. SPIE Int. Soc. Opt. Eng.*, **4514**, 82 (2001).
13. Balakshy V.I., Slivin'ski A., Tolpin K.A. *Opt. Spektrosk.*, **87**, 1003 (1999).